

Research Article

Rootlike Morphology of ZnO:Al Thin Film Deposited on Amorphous Glass Substrate by Sol-Gel Method

Heri Sutanto,¹ Sufwan Durri,¹ Singgih Wibowo,¹ Hady Hadiyanto,² and Eko Hidayanto¹

¹Department of Physics, Faculty of Science and Mathematics, Diponegoro University, Jalan Prof. Soedarto SH Street, Tembalang, Semarang 50275, Indonesia

²Department of Chemical Engineering, Faculty of Engineering, Diponegoro University, Jalan Prof. Soedarto SH Street, Tembalang, Semarang 50275, Indonesia

Correspondence should be addressed to Heri Sutanto; herisutanto@undip.ac.id

Received 2 March 2016; Revised 25 April 2016; Accepted 9 May 2016

Academic Editor: Lorenzo Pavesi

Copyright © 2016 Heri Sutanto et al. This is an open access article distributed under the Creative Commons Attribution License, which permits unrestricted use, distribution, and reproduction in any medium, provided the original work is properly cited.

Zinc oxide (ZnO) and aluminum doped zinc oxide (ZnO:Al) thin films have been deposited onto a glass substrate by sol-gel spray coating method at atmospheric pressure. X-ray diffractometer (XRD), scanning electron microscopy (SEM), and UV-Vis spectrophotometer have been used to characterize the films. XRD spectra indicated that all prepared thin films presented the wurtzite hexagonal structure. SEM images exhibited rootlike morphology on the surface of thin films and the shortest root diameter was about $0.219\ \mu\text{m}$. The UV-Vis absorption spectra exhibited the absorption edges that were slightly shifted to the lower wavelength. From this result, the incorporation of aluminum into the ZnO involved a slight increase in the optical band-gap of films. The optical bands of films were 3.102 eV, 3.115 eV, 3.118 eV, 3.115 eV, 3.109 eV, and 3.109 eV for ZnO, ZnO:Al 2%, ZnO:Al 4%, ZnO:Al 6%, ZnO:Al 8%, and ZnO:Al 10%, respectively. Increase of Al doping concentration in ZnO films contributed to the increase of their optical band-gap which can be explained by the Burstein-Moss effect.

1. Introduction

Zinc oxide (ZnO) is the most popular materials that can be used for many applications. Many researchers have studied this material for electronics [1], energy [2], and environment [3] applications. ZnO is of low cost and nontoxic and has high chemical stability which make this material so interesting [4]. ZnO can be used for transparent conductive oxide [5], gas sensors [6], and photocatalyst [7–9]. ZnO has a wide band-gap energy ($\sim 3.3\ \text{eV}$) and has been studied in different forms such as powder [10] and thin film [11]. Several techniques can be used to make ZnO:Al thin film, such as DC or RF magnetron sputtering [12, 13], electron beam evaporation [14], pulsed laser deposition [15], chemical vapor deposition [16], spray pyrolysis [17], and sol-gel processing [18]. Sol-gel is the most widely used method because of its easy and low-cost preparation [19].

Substitution of Zn^{2+} ion by group III ions such as B^{3+} , Al^{3+} , Ga^{3+} , and In^{3+} will produce extra electrons and improve optical, electrical, thermal, and magnetic properties. The

most commonly used dopant is aluminum (Al) [20, 21]. In this work, we proposed ZnO and ZnO:Al thin films deposited by sol-gel spray coating. The films have been characterized by XRD, SEM-EDX, and UV-Vis. The Al doping concentration in the ZnO:Al films was controlled and its effect on the films properties was investigated.

2. Materials and Method

ZnO and ZnO:Al thin films were synthesized by sol-gel spray coating method. As a starting material, zinc acetate dihydrate ($\text{Zn}(\text{CH}_3\text{COO})_2 \cdot 2\text{H}_2\text{O}$) was dissolved in 2-propanol with a concentration of $0.5\ \text{mol L}^{-1}$. Monoethanolamine (MEA) was wisely dropped into solution and was stirred under room temperature for 30 min. For doped films, aluminum nitrate nonahydrate ($\text{Al}(\text{NO}_3)_3 \cdot 9\text{H}_2\text{O}$) was added to the solution with a molar percentage, fixed at 0, 2, 4, 6, 8, and 10% moles and were then denoted as ZnO, ZA2, ZA4, ZA6, ZA8, and ZA10, respectively. The precursor solution was deposited onto glass substrate by spray coating at 450°C hotplate temperature

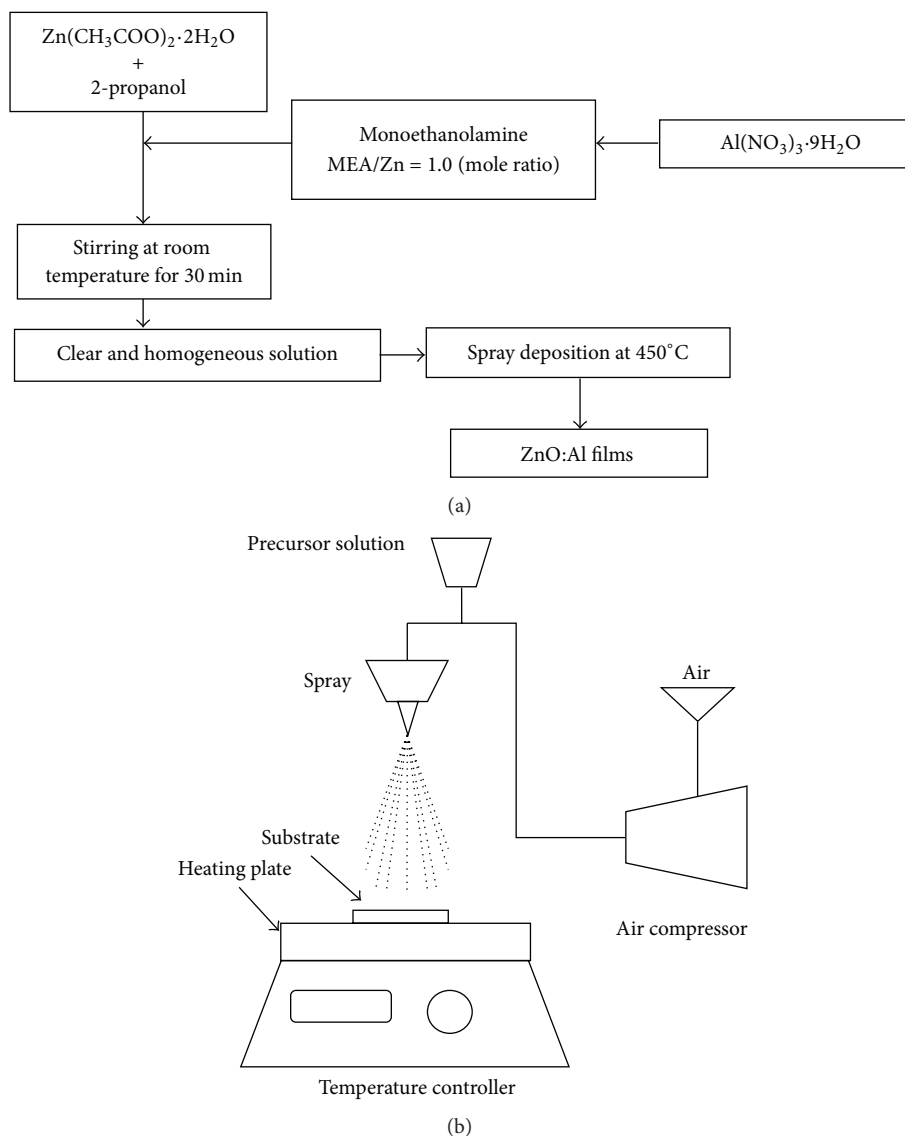


FIGURE 1: (a) The flow chart shows ZnO:Al preparation by sol-gel technique. (b) Diagram of spray coating system.

and allowed for 1 hr. Figure 1(a) showed the flow chart of preparation and (b) diagram of spray coating system that was used in this study. Prior to a deposition, the glass substrate was cleaned by ultrasonic cleaner using acetone, methanol, and bidistilled water. The prepared thin films were characterized by X-ray diffraction (XRD) using Shimadzu Maxima 7000 (Cu-K α wavelength: 1.5405 Å). The detection angles were ranging from $2\theta = 10$ to 90° . The morphology of thin films was shown by scanning electron microscopy (SEM) and energy dispersive X-ray spectroscopy (EDX) using JEOL-JSM 6510 LA. The optical transmission of the films was measured by a UV-Vis spectrophotometer (Shimadzu 1240 SA).

3. Results and Discussion

3.1. Microstructure. Figure 2 depicts the polycrystalline diffraction pattern for all prepared samples. The pattern

clearly showed the hexagonal wurtzite structure of ZnO and matched with the reported data on JCPDS 36-1451. The pattern also demonstrates that the obtained thin films have sharp and narrow peaks, indicating that the materials exhibit high crystallinity. The high crystallinity film can be achieved on amorphous glass surface under high temperature deposition. In our deposition method, the hotplate temperature was adjusted at 450°C which enable making polycrystalline of ZnO. In the ZnO:Al spectra, only ZnO phase was detected and there is no Al or Al oxide phase. This result suggests that the thin films do not have any phase segregation or secondary phase formation because of Al incorporation into ZnO lattice. It also might be caused by Al content which was so small to be detected. We can see that ZA4 and ZA10 exhibited amorphicity due to the glass substrate. The pattern also demonstrates a preferential *c*-axis-orientated structure with the most intense peak at (002). This preferential growth is dependent on the deposition temperature. Ali et al. [22]

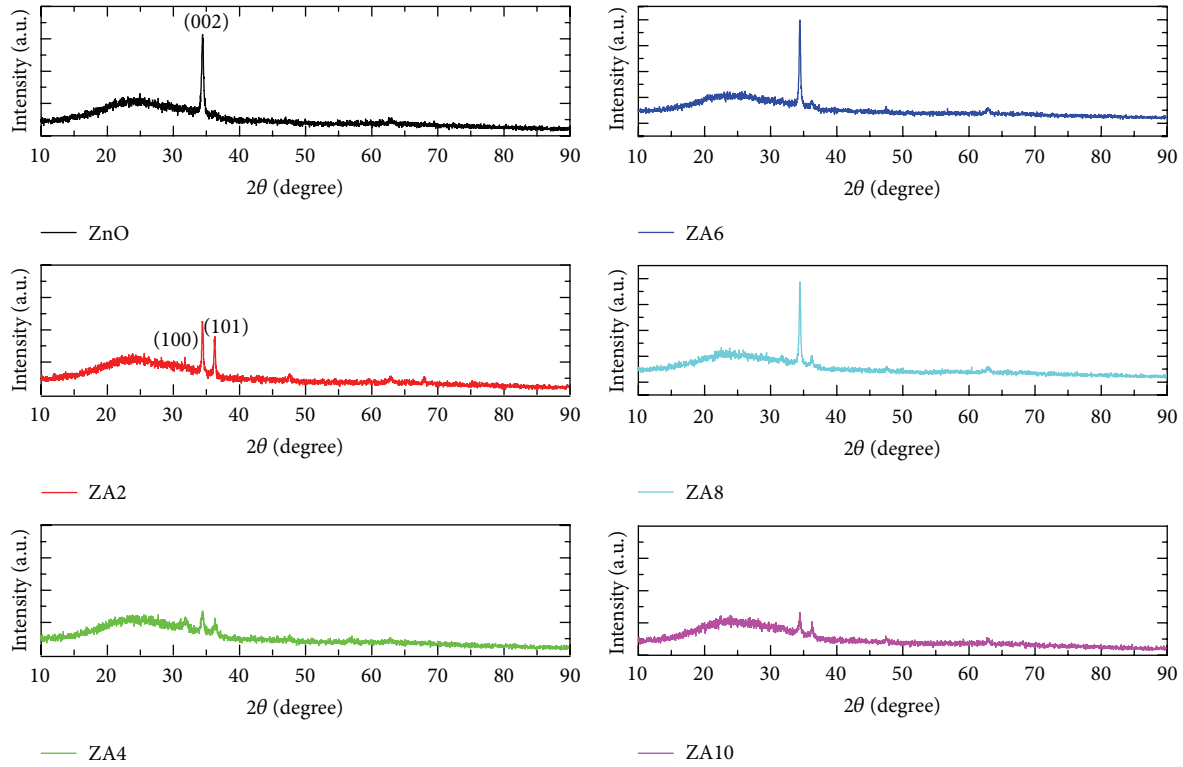


FIGURE 2: XRD spectra of ZnO and ZnO:Al thin films.

have reported that the optimal growth temperature for the RF-sputtering technique was 400°C. In our study with a sol-gel method and a small temperature difference, we still get high quality of polycrystalline of ZnO:Al. The crystallite size can be estimated by the Scherrer formula (see equation (1)) using (002) peak. The crystallite size of ZnO:Al became bigger than pure ZnO thin film and is shown in Table 1:

$$D = \frac{k\lambda}{\beta_{1/2} \cos \theta}, \quad (1)$$

where $k = 0.90$ is the Scherrer constant, $\beta_{1/2}$ is the full width at half maximum and $\lambda = 1.5405 \text{ \AA}$ is the wavelength of Cu-K α radiation.

We can note that the lattice parameter c decreased; it might be affected by the substitutional replacement of Zn^{2+} (ionic radius 0.072 nm) ions by Al^{3+} (ionic radius 0.053 nm) [23]. The estimated value of crystallite size from (002) plane was found to increase from 18.85 nm for ZnO to 25.37 nm for ZA10. Normally, it was expected that the crystallite size should also decrease due to replacement of Zn^{2+} ions by Al^{3+} ions [24]. The same result has been obtained by Abd-Lefdil et al. [25]. The increase in crystallite size may be due to the enhanced thickness of Al-doped films. During deposition process, the lower surface energy grains may become larger as film thickness increase [26].

3.2. Morphology. Figure 3 represents the SEM observation of all prepared samples. It can be seen that all films have rootlike morphology. In ZnO image, the root surface had the longest

TABLE 1: FWHM and crystallite size parameters of thin films.

Sample name	2θ (002)	FWHM (deg)	D (nm)	c (Å)
ZnO	34.42	0.45816	18.85	5.206797
ZA2	34.48	0.36741	23.52	5.198011
ZA4	34.42	0.44695	19.33	5.206797
ZA6	34.44	0.33876	25.50	5.203865
ZA8	34.42	0.34697	24.90	5.206797
ZA10	34.44	0.34048	25.37	5.203865

diameter of all other samples. ZnO:Al thin films had shorter root diameter and the shortest root diameter was obtained by ZA6. The root diameter was shown in Table 2. The rootlike morphology was rarely found in other ZnO thin film studies.

Figure 4 depicts the suggested ZnO growth mechanism using sol-gel spray coating method at 450°C. During deposition, the layer of crystalline grains is built onto glass substrate. There is a different temperature from the first layer and other layers that affects the interaction among them. Many particles merge with other particles to make a long structure of ZnO which is called rootlike morphology.

EDX result exhibited Al composition in the thin film sample which was different from Al composition in the precursor solution as shown in Table 2. This might be caused by only a small percentage of Al ions that enable substituting Zn ion. Another reason was the high loss of Al during spray deposition. We can see the saturation result of Al/Zn incorporation at higher percentage of Al doping. This result

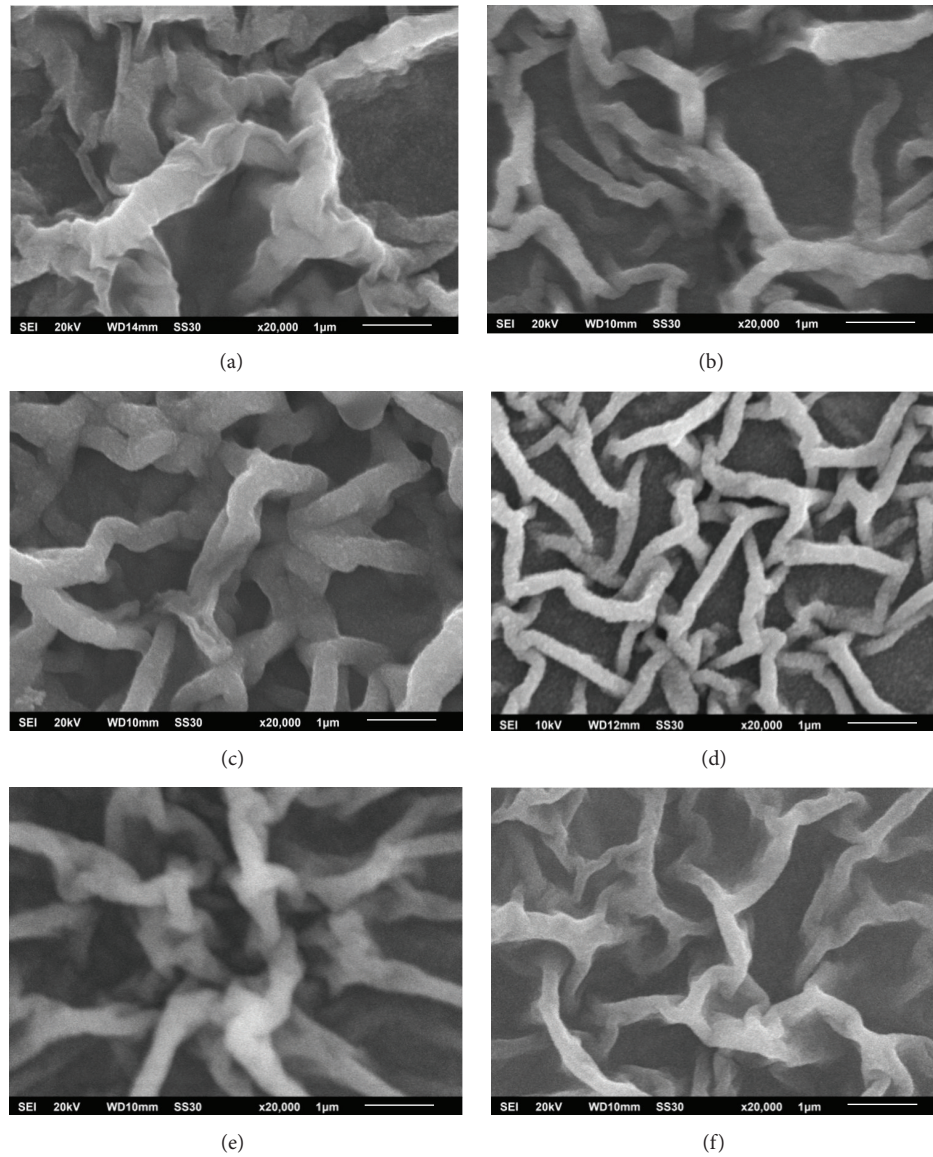


FIGURE 3: SEM images of ZnO (a), ZA2 (b), ZA4 (c), ZA6 (d), ZA8 (e), and ZA10 (f) thin films.

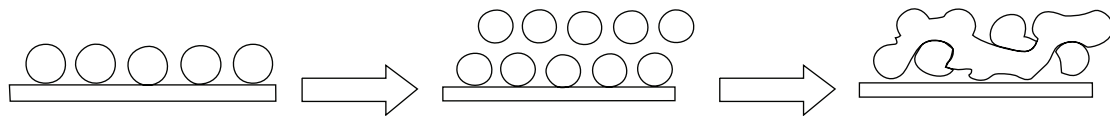


FIGURE 4: Rootlike morphology of ZnO:Al mechanism.

TABLE 2: Root diameter, Al/Zn composition, and energy gap of thin films.

Sample name	Root diameter (μm)	Al/Zn in solution	Al/Zn incorporated	Energy gap (eV)
ZnO	0.482	0	0	3.102
ZA2	0.227	0.02	0.01	3.115
ZA4	0.377	0.04	0.02	3.118
ZA6	0.219	0.06	0.03	3.115
ZA8	0.375	0.08	0.03	3.109
ZA10	0.288	0.10	0.03	3.109

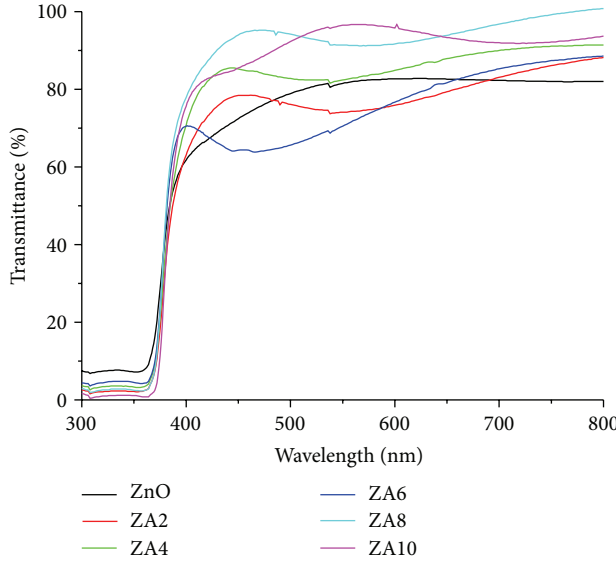


FIGURE 5: Optical transmittance spectra of thin films.

was affected by the limitation of Al doping in ZnO thin film. The thermodynamic solubility limit of Al in ZnO has been reported to be in the 2-3 at. % range [27]. According to the phase diagram of Al/Zn mixture in the previous study [28], the mixture only shows Zn phase at our temperature treatment. The limitation of Al is the maximum Al content in the ZnO at a given temperature. The substitution of Al in ZnO remains quite difficult because of the difference in ionic radius, coordination preference, and oxidation state [29].

3.3. Optical Properties. The optical transmittance spectra were shown in Figure 5 and, in these spectra, an improvement of the film transparency at high Al doping concentration can be seen. The highest transparency was obtained by ZA8 about 95% in the visible wavelength region. The increase can be explained by the reduction of light scattering in the film which was caused by the lower thickness [18]. It also exhibited the fringes pattern that indicated the high quality and homogenous surface [30]. Figure 6 shows the absorbance spectra of all prepared thin films. We can see that ZnO:Al thin films have a slight shift to lower wavelength (blue shift).

The optical band-gap can be estimated from the transmission spectra. Prior to calculation, the absorption coefficient should be calculated using the formula below:

$$\alpha = \ln\left(\frac{1}{T}\right) \times \left(\frac{1}{e}\right), \quad (2)$$

where T is the transmittance spectra and e is the thickness of the thin film. We can use α from the calculation to get the optical band-gap and obey the following equation:

$$(\alpha h\nu)^2 = A(h\nu - E_g), \quad (3)$$

where α is the absorption coefficient, $h\nu$ is the photon energy, A is a constant, and E_g is the optical band-gap [31]. The optical band-gap E_g can be obtained by extrapolating the linear part of the curve to $(\alpha h\nu)^2 = 0$ if one plots $(h\nu)^2 \sim h\nu$.

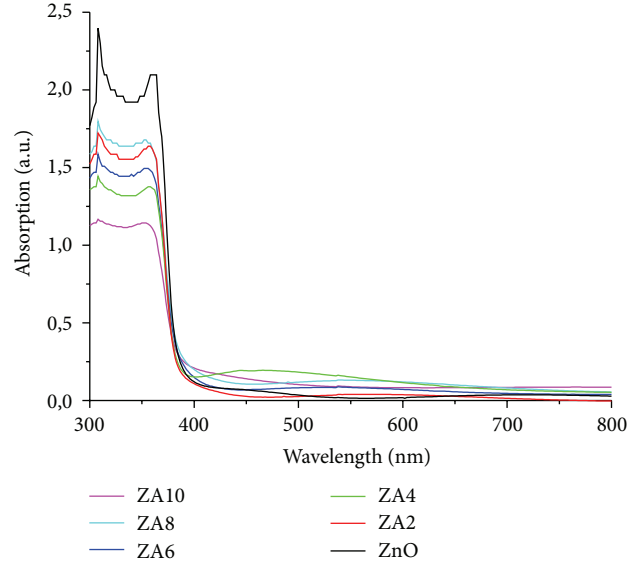


FIGURE 6: Absorbance spectra of thin films.

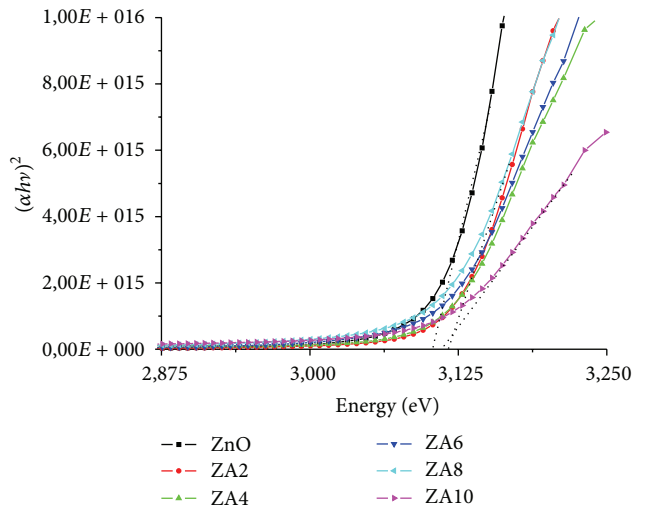


FIGURE 7: Optical band-gap of thin films.

The optical band-gap of ZnO and ZnO:Al thin film was presented in Figure 7. The ZnO:Al thin films had bigger optical band-gap than pure ZnO thin film; the same result has been obtained by some papers [32–35]. The increase of band-gap was caused by the Moss-Burstein effect [36]. The effect stated that the blue shift of the optical band-gap of semiconductors is affected by impurity in the conduction band [37]. ZnO:Al films are semiconductors in which the Fermi level lies in the conduction band which means that electrons occupy the levels at the bottom of the conductivity band [37, 38].

4. Conclusions

The pure and the aluminum doped ZnO films were successfully deposited by the sol-gel spray coating technique. XRD

spectra showed the hexagonal wurtzite structure of ZnO. The estimated crystallite size increases with addition of Al due to replacement of Zn^{2+} ions by Al^{3+} ions. The surface of all prepared thin films showed rootlike morphology and the diameter decreased with increase of Al content. The transmittance spectra showed high transparency of ZnO:Al thin films about 95%. The absorbance spectra exhibited that ZnO:Al had a slight shift to higher wavelength than pure ZnO. The optical band-gap resulted in slight increase for the Al-doped films as explained by the Moss-Burstein effect.

Competing Interests

The authors declare that there is no conflict of interests regarding the publication of this paper.

Acknowledgments

The authors would like to thank The Ministry of Research, Technology and Higher Education, Indonesia, through Competence Grant 2016 for funding of this work.

References

- [1] L. Znaidi, T. Touam, D. Vrel et al., "ZnO thin films synthesized by sol-gel process for photonic applications," *Acta Physica Polonica A*, vol. 121, no. 1, pp. 165–168, 2012.
- [2] C.-P. Lee, C.-Y. Chou, C.-Y. Chen et al., "Zinc oxide-based dye-sensitized solar cells with a ruthenium dye containing an alkyl bithiophene group," *Journal of Power Sources*, vol. 246, pp. 1–9, 2014.
- [3] H. Sutanto, I. Nurhasanah, and E. Hidayanto, "Deposition of Ag 2~6 mol%-doped ZnO photocatalyst thin films by thermal spray coating method for *E.coli* bacteria degradation," *Materials Science Forum*, vol. 827, pp. 3–6, 2015.
- [4] A. Sharma and P. Sanjay Kumar, "Synthesis and characterization of CeO-ZnO nanocomposites," *Nanoscience and Nanotechnology*, vol. 2, no. 3, pp. 82–85, 2012.
- [5] Y. Liu, Y. Li, and H. Zeng, "ZnO-based transparent conductive thin films: doping, performance, and processing," *Journal of Nanomaterials*, vol. 2013, Article ID 196521, 9 pages, 2013.
- [6] A. B. Kashyout, H. M. A. Soliman, H. S. Hassan, and A. M. Abousehly, "Fabrication of ZnO and ZnO:Sb nanoparticles for gas sensor applications," *Journal of Nanomaterials*, vol. 2010, Article ID 341841, 8 pages, 2010.
- [7] G. Kenanakis and N. Katsarakis, "Ultrasonic spray pyrolysis growth of ZnO and ZnO:Al nanostructured films: application to photocatalysis," *Materials Research Bulletin*, vol. 60, no. 1, pp. 752–759, 2014.
- [8] S. Wibowo and H. Sutanto, "Preparation and characterization of double layer thin films ZnO/ZnO:Ag for methylene blue photodegradation," *AIP Conference Proceedings*, vol. 1710, pp. 0300491–0300495, 2016.
- [9] H. Sutanto, I. Nurhasanah, E. Hidayanto, S. Wibowo, and Hadiyanto, "Synthesis and characterization of ZnO:TiO₂ nano composites thin films deposited on glass substrate by sol-gel spray coating technique," *AIP Conference Proceedings*, vol. 1699, Article ID 040005, pp. 1–7, 2015.
- [10] C. C. Chen, P. Liu, and C. H. Lu, "Synthesis and characterization of nano-sized ZnO powders by direct precipitation method," *Chemical Engineering Journal*, vol. 144, no. 3, pp. 509–513, 2008.
- [11] T. Ivanova, A. Harizanova, T. Koutzarova, and B. Vertruyen, "Optical characterization of sol-gel ZnO:Al thin films," *Superlattices and Microstructures*, vol. 85, pp. 101–111, 2015.
- [12] D.-S. Kim, J.-H. Park, B.-K. Shin et al., "Effect of deposition temperature on the properties of Al-doped ZnO films prepared by pulsed DC magnetron sputtering for transparent electrodes in thin-film solar cells," *Applied Surface Science*, vol. 259, pp. 596–599, 2012.
- [13] W. F. Yang, Z. G. Liu, D.-L. Peng et al., "Room-temperature deposition of transparent conducting Al-doped ZnO films by RF magnetron sputtering method," *Applied Surface Science*, vol. 255, no. 11, pp. 5669–5673, 2009.
- [14] D. R. Sahu, S.-Y. Lin, and J.-L. Huang, "Improved properties of Al-doped ZnO film by electron beam evaporation technique," *Microelectronics Journal*, vol. 38, no. 2, pp. 245–250, 2007.
- [15] Y. D. Liu and J. S. Lian, "Optical and electrical properties of aluminum-doped ZnO thin films grown by pulsed laser deposition," *Applied Surface Science*, vol. 253, no. 7, pp. 3727–3730, 2007.
- [16] Y. Natsume, H. Sakata, T. Hirayama, and H. Yanagida, "Low-temperature conductivity of ZnO films prepared by chemical vapor deposition," *Journal of Applied Physics*, vol. 72, no. 9, pp. 4203–4207, 1992.
- [17] A. J. C. Fiddes, K. Durose, A. W. Brinkman, J. Woods, P. D. Coates, and A. J. Banister, "Preparation of ZnO films by spray pyrolysis," *Journal of Crystal Growth*, vol. 159, no. 1–4, pp. 210–213, 1996.
- [18] X. Liu, K. Pan, W. Li, D. Hu, S. Liu, and Y. Wang, "Optical and gas sensing properties of Al-doped ZnO transparent conducting films prepared by sol-gel method under different heat treatments," *Ceramics International*, vol. 40, no. 7, pp. 9931–9939, 2014.
- [19] H. Sutanto, S. Wibowo, I. Nurhasanah, E. Hidayanto, and H. Hadiyanto, "Ag doped ZnO thin films synthesized by spray coating technique for methylene blue photodegradation under UV irradiation," *International Journal of Chemical Engineering*, vol. 2016, Article ID 6195326, 6 pages, 2016.
- [20] A. Alkahlout, "A comparative study of spin coated transparent conducting thin films of gallium and aluminum doped ZnO nanoparticles," *Physics Research International*, vol. 2015, Article ID 238123, 8 pages, 2015.
- [21] A. Al Kahlout, N. Al Dahoudi, S. Heusing, K. Moh, R. Karos, and P. W. De Oliveira, "Structural, electrical and optical properties of aluminum doped zinc oxide spin coated films made using different coating sols," *Nanoscience and Nanotechnology Letters*, vol. 6, no. 1, pp. 37–43, 2014.
- [22] A. I. Ali, C. H. Kim, J. H. Cho, and B. G. Kim, "Growth and characterization of ZnO:Al thin film using RF sputtering for transparent conducting oxide," *Journal of the Korean Physical Society*, vol. 49, no. 2, pp. S652–S656, 2006.
- [23] E. Bacaksiz, S. Aksu, S. Yilmaz, M. Parlak, and M. Altunbaş, "Structural, optical and electrical properties of Al-doped ZnO microrods prepared by spray pyrolysis," *Thin Solid Films*, vol. 518, no. 15, pp. 4076–4080, 2010.
- [24] A. Mahroug, S. Boudjadar, S. Hamrit, and L. Guerbous, "Structural, optical and photocurrent properties of undoped and Al-doped ZnO thin films deposited by sol-gel spin coating technique," *Materials Letters*, vol. 134, pp. 248–251, 2014.

- [25] M. Abd-Lefdil, A. Douayar, A. Belayachi et al., "Third harmonic generation process in Al doped ZnO thin films," *Journal of Alloys and Compounds*, vol. 584, pp. 7–12, 2014.
- [26] S. Mondal, S. R. Bhattacharyya, and P. Mitra, "Effect of Al doping on microstructure and optical band gap of ZnO thin film synthesized by successive ion layer adsorption and reaction," *Pramana*, vol. 80, no. 2, pp. 315–326, 2013.
- [27] M. H. Yoon, S. H. Lee, H. L. Park, H. K. Kim, and M. S. Jang, "Solid solubility limits of Ga and Al in ZnO," *Journal of Materials Science Letters*, vol. 21, no. 21, pp. 1703–1704, 2002.
- [28] Y. H. Zhu, "General rule of phase decomposition in Zn-Al based alloys (II)-on effects of external stresses on phase transformation," *Materials Transactions*, vol. 45, no. 11, pp. 3083–3097, 2004.
- [29] H. Serier, M. Gaudon, and M. Ménétrier, "Al-doped ZnO powdered materials: Al solubility limit and IR absorption properties," *Solid State Sciences*, vol. 11, no. 7, pp. 1192–1197, 2009.
- [30] S. Ilican, M. Caglar, and Y. Caglar, "Determination of the thickness and optical constants of transparent indium-doped ZnO thin films by the envelope method," *Materials Science-Poland*, vol. 25, no. 3, pp. 709–718, 2007.
- [31] M. Mazilu, N. Tigau, and V. Musat, "Optical properties of undoped and Al-doped ZnO nanostructures grown from aqueous solution on glass substrate," *Optical Materials*, vol. 34, no. 11, pp. 1833–1838, 2012.
- [32] S. M. Rozati and S. Akestehteh, "Characterization of ZnO:Al thin films obtained by spray pyrolysis technique," *Materials Characterization*, vol. 58, no. 4, pp. 319–322, 2007.
- [33] J. J. Ding, S. Y. Ma, H. X. Chen, X. F. Shi, T. T. Zhou, and L. M. Mao, "Influence of Al-doping on the structure and optical properties of ZnO films," *Physica B: Condensed Matter*, vol. 404, no. 16, pp. 2439–2443, 2009.
- [34] M. Bizarro, A. Sánchez-Arzate, I. Garduño-Wilches, J. C. Alonso, and A. Ortiz, "Synthesis and characterization of ZnO and ZnO:Al by spray pyrolysis with high photocatalytic properties," *Catalysis Today*, vol. 166, no. 1, pp. 129–134, 2011.
- [35] B. E. Sernelius, K.-F. Berggren, Z.-C. Jin, I. Hamberg, and C. G. Granqvist, "Band-gap tailoring of ZnO by means of heavy Al doping," *Physical Review B*, vol. 37, no. 17, pp. 10244–10248, 1988.
- [36] M.-I. Lee, M.-C. Huang, D. Legrand, G. Lerondel, and J.-C. Lin, "Structure and characterization of Sn, Al co-doped zinc oxide thin films prepared by sol-gel dip-coating process," *Thin Solid Films*, vol. 570, pp. 516–526, 2014.
- [37] T. S. Moss, "The interpretation of the properties of indium antimonide," *Proceedings of the Physical Society. Section B*, vol. 67, no. 10, article 775, 1954.
- [38] Y. Ammaih, A. Lfakir, B. Hartiti, A. Ridah, P. Thevenin, and M. Siadat, "Structural, optical and electrical properties of ZnO:Al thin films for optoelectronic applications," *Optical and Quantum Electronics*, vol. 46, no. 1, pp. 229–234, 2014.

